

## HETGS

**Norbert S. Schulz, for the HETGS team**

### Performance, Calibration, and Software

During Cycle 16 and the first part of Cycle 17 the High Energy Transmission Gratings Spectrometer (HETGS) continued to perform nominally. There were 24 targets observed in Cycle 16 in 50 separate observations for a total exposure of 2.5 Ms. This total exposure is very similar to previous *Chandra* cycles and demonstrates that the HETGS is the instrument of choice for spectroscopy, only second to ACIS-S3, which is the main instrument for imaging spectroscopy onboard *Chandra*. Single exposures ranged from 4 to 138 ks with 43 observations in timed event mode and 7 observations in continuous clocking mode. The latter were very bright black hole binary targets exhibiting exceptionally high count rates in the HETG 1st orders of up to 300 cts/s. The target selection was very diverse and included low mass stars, high mass stars, cataclysmic binaries, low-mass neutron star binaries, high mass X-ray binaries, black hole binaries, supernovae, blazars, and active galactic nuclei.

Of these observations three were designated calibration observations. Observations of MKN 421 and 3C273 were performed to monitor the contaminant on the ACIS-S filters. Of specific importance were high amplitude (512 rows) dither observations of MKN 421 at low and high chip locations, which will allow for measurements of the contaminant over a large area of the ACIS spectroscopic array and maps of variations in the contaminant thickness across the array. Unfortunately it appears that the contaminant is accumulating at a fast rate, which is stimulating discussions amongst various groups on attempts to remove significant portions of the contaminant through a bakeout procedure.

The HETGS data were not subject to major changes with respect to calibration or analysis software except for a new order sorting treatment for CC-mode. We now calculate the y-coordinate in order to apply the correct gain and CTI corrections. New releases of CIAO (4.8.1) and CALDB (4.7.1) went into effect by the beginning of this year to accommodate changes in the flight grades that were included for observations taken after November 2009 and to modify quantum efficiencies for CC-GRADED mode observations taken before that date. As it turned out, the inclusion of flight

grade G66 events in these observations introduced spurious background events to the spectra below  $\sim 1$  keV. This means that for observations dated after November 2009 observers should filter out flight grade G66 events from the EVT2 file and re-extract PHA2 spectra until the issue is corrected in an upcoming CALDB release. The modified quantum efficiencies will then be valid for all CC-GRADED mode observations. A corresponding thread can be found at the CIAO CC mode page: (<http://cxc.harvard.edu/ciao>).

### Selected Scientific Highlights

The science output for the HETGS still reflects a high level of quality. Many papers went into press in the past year highlighting a variety of science topics. The data used included a good mix of new and recent observations, but also many previous cycles from the *Chandra* archive. Topics included accretion disk winds in GRS 1915+105 (Miller et al. 2016), probing Wolf-Rayet winds in WR6 (Huenemoerder et al. 2015), Compton-thick states in NGC 1365 (Nardini et al. 2015), a giant outburst of V404 Cygni (King et al. 2015), X-ray properties of low-mass pre-main sequence stars in the Orion Nebula Cluster (Schulz et al. 2015), a review of the 3.5 keV line in Galaxy Clusters (Phillips et al. 2015), simultaneous observations with NUSTAR of the bursting pulsar GRO J1744-28 (Younes et al. 2015), as well as X-rays from a pole-dominated corona on AB Dor (Drake et al. 2015) to name a few. The following sections highlight some of the science content in more detail.

### Si K $\alpha$ Emissions

Early *Chandra* observations of ionized winds such as in Vela X-1, 4U 1700-37, and, more recently, Cyg X-1 detected Si and S K $\alpha$  emissions from O-, C-, Li-, B-, and Be-like ions. While highly ionized ions from Si, such as the He-like triplet Si XIII with only two electrons left and the H-like ions with only one electron left, are readily observed in a variety of astrophysical X-ray emitting plasmas, these K $\alpha$  emissions from Si II to Si XII are more rare and stem from cooler and more dense plasma sites. These states have been observed primarily from HMXBs, such as Vela X-1 in eclipse (Schulz et al. 2002) and out of eclipse (Watanabe et al. 2006), 4U 1700-37 (Boroson et al. 2003) and Cyg X-1 (Miskovicova et al. 2016), to name the most prominent examples, but also in the Seyfert 2 galaxy NGC 1068 (Kallman et al. 2014). These emissions (and absorptions) are important diagnostics of the emitting

plasma state that can distinguish colder, less ionized plasmas and denser more clumped plasmas from hot coronal plasmas. However, reference atomic data on these states have been surprisingly absent and unambiguous conclusions have been impossible because of the relatively poor accuracy of the calculations. For a long time one had to rely on the Hartree-Fock calculations by House (1969) until the semi-relativistic Hartree-Fock calculations by Palmeri et al. (2008). More recently, Natalie Hell and collaborators from the Lawrence Livermore Laboratories measured these states in situ for He- to Ne-like Si and S ions with an accuracy of better than 1 eV with the electron beam ion traps (EBIT-1, SuperEBIT, and the NASA/GSFC EBIT Calorimeter; Hell et al. 2016). Figure 1 shows a comparison of the out of eclipse Vela X-1 Si spectral region as observed by the *Chandra* HETGS to the laboratory EBIT calorimeter spectrum. All these analyses were performed using the Interactive Spectral Interpretation System ISIS (<http://space.mit.edu/ASC/ISIS>) as provided by MIT/CXC (see also Noble & Nowak 2008 and references therein).

### The Spin-Orbit Split in Fe XXVI Transitions

The HETGS provides superb spectral resolution throughout the soft X-ray band (0.2 and 10 keV). The spectral resolution in the first order of the High Energy Gratings (HEG) spectra is 0.011 Å which corresponds to a resolving power of 180 in the Fe K region and almost 1200 in the O K region. Even better resolution can be achieved by using higher orders. The HEG gratings are optimized to support odd numbered orders and in third order can reach up to 10% efficiency at a resolving power of 540, however, at the expense of bandpass, which, in this case, ranges from 1.5 Å to about 10 Å. For the Fe K region this leads to a resolution of roughly 13 eV, which is sufficient to resolve the spin-orbit coupling in the H-like transitions of Fe XXVI ions that has an energy shift of 21.2 eV. A study of wind absorption in bright black hole binaries by Miller et al. (2015) did just that. Figure 2 shows HEG third order spectra of the Fe K region of four such binaries. Absorptions in these binaries differ depending on the physical properties of the absorber and, at least in the case of GRO J1655-40, the conditions are good enough to see the two spin-orbit split line components for a static absorber (red lines) and a dynamic and thus blue-shifted absorber (blue lines). The split components do not show the atomic ratio of

2:1 because absorption appears saturated, which gives the observer additional clues about column densities in the curve of growth. The data at high resolution also show skewed absorption profiles in Fe XXV showing sensitivity to the very weak absorbing power of the intercombination line component. The forbidden line cannot be observed in absorption because it does not have a measurable electric dipole moment. This study nicely highlights the power of spectral resolution to study astrophysical X-ray plasmas.

### The Orion Nebula Cluster

The Orion Trapezium stars at the heart of the Orion Nebula Cluster (ONC) provide a perfect laboratory to study the early evolution of very young and diverse stars. The HETGS Orion Legacy Project at MIT accumulated 585 ks of predominantly guaranteed time (GTO) exposure centered on the Orion Trapezium and analyzed the brightest spectra in the HETGS field of view leading to more than half a dozen of papers to date. While these studies focused entirely on the massive and intermediate mass stars, the latest study highlights X-ray spectral emissions from very young low-mass pre-main sequence stars. Figure 3 shows four HETGS spectra from the stellar sample. The study of

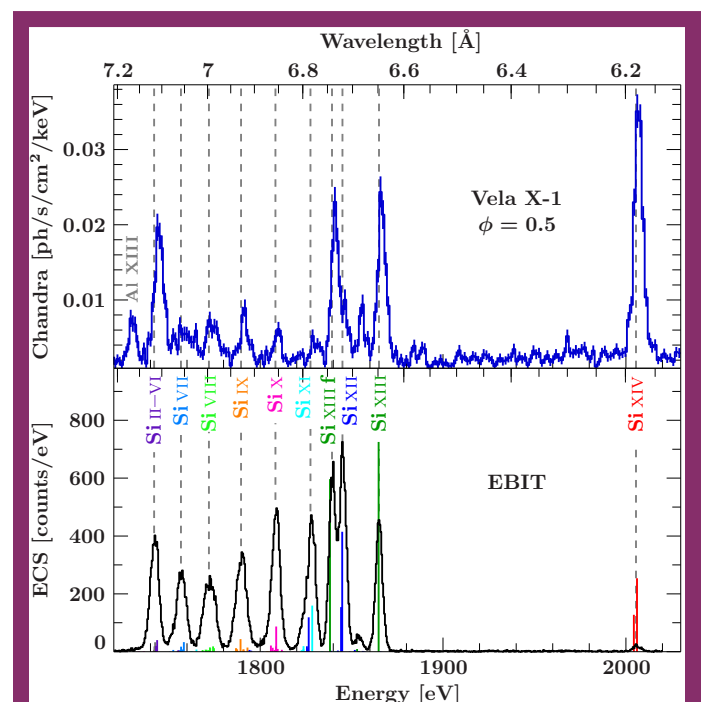


Figure 1: Comparison of the spectral regions for silicon as observed by the *Chandra* HETGS in Vela X-1 out of eclipse (OBSID 1927) to the one measured in the laboratory by EBIT (from Hell et al. 2016). Si K $\alpha$  emission can now be benchmarked to a precision better than 1 eV.

six stars finds that the spectra are fit by two temperature plasmas with dominating high temperatures of about 40 MK. It was concluded that based on the line ratios no further temperature components were needed thus constraining the differential emission measure distribution to two major peaks as predicted by previous lower resolution studies. The total emission measures as well as abundances were comparable to active coronal sources. The stellar surface X-ray flux also correlated well with stellar age within the age range of 0.1 and 10 Myr, signaling a rapid increase of coronal activity in these stars during their young growth. These results demonstrated the power of X-ray line diagnostics to study coronal properties of T Tauri stars in young stellar clusters.

### Probing Wolf-Rayet Winds

In contrast to these low-mass PMS stars, the most massive and luminous stars in the Milky Way, even though they are not much older in age, are already close to the end of their life cycle and exhibit fundamentally different X-ray properties. These Wolf-Rayet stars, which eventually will end in a core-collapse supernova detonation, are characterized by rapid outflows that enrich and energize the interstellar medium (see Huenemoerder et al. 2015 for details). Highly resolved X-ray emissions from these stars are still rare to date and the study by Huenemoerder et al. (2015) illustrates some extraordinary stellar wind emissions. The unusual strength of the He-like forbidden lines relative to their normal early type cousins places the source of the X-ray emissions at tens to hundreds of stellar radii from the photosphere. In O-star winds, however, this is not the case, and it appears that we are looking through a much thinner wind almost down to the photosphere. There is also a significant amount of random variability in the emissions, which is usual for early type stars. Figure 4 (on the next page) shows unusual “fin”-shaped line profiles for some of the unblended lines. Line ratios and the heavily skewed line profiles show that the outflow is optically thick with optical depths well above unity resulting in the heavily absorbed red flanks of the line profiles. This study will help pave the way to a more fun-

damental theoretical understanding of stellar winds in massive stars (Huenemoerder et al. 2015). ■

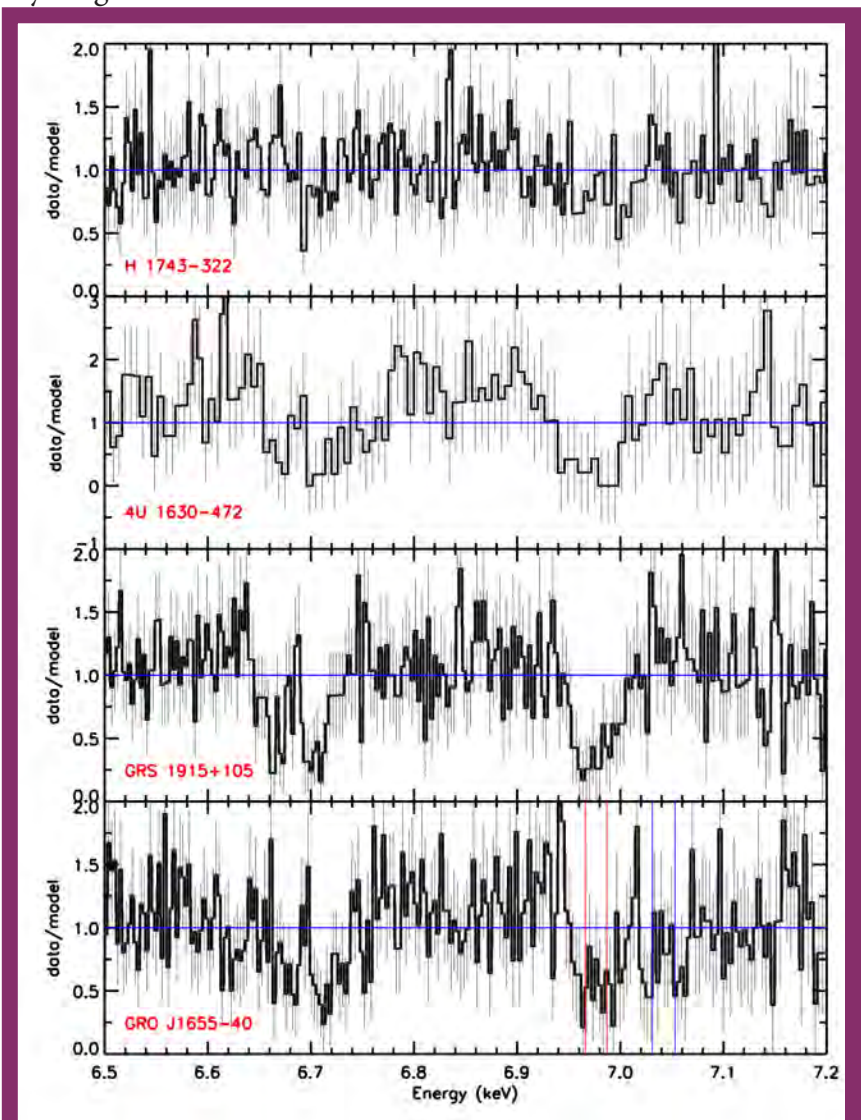


Figure 2: The Fe K region in four black hole X-ray binaries observed with the high energy gratings (HEG) in third order (from Miller et al. 2015). Some show spurious, some show well developed line absorption from stellar winds. These 3rd order spectra have a spectral resolution of 13 eV allowing the observation spin-orbit multiplets in the Fe XXVI transitions (see red and blue lines).

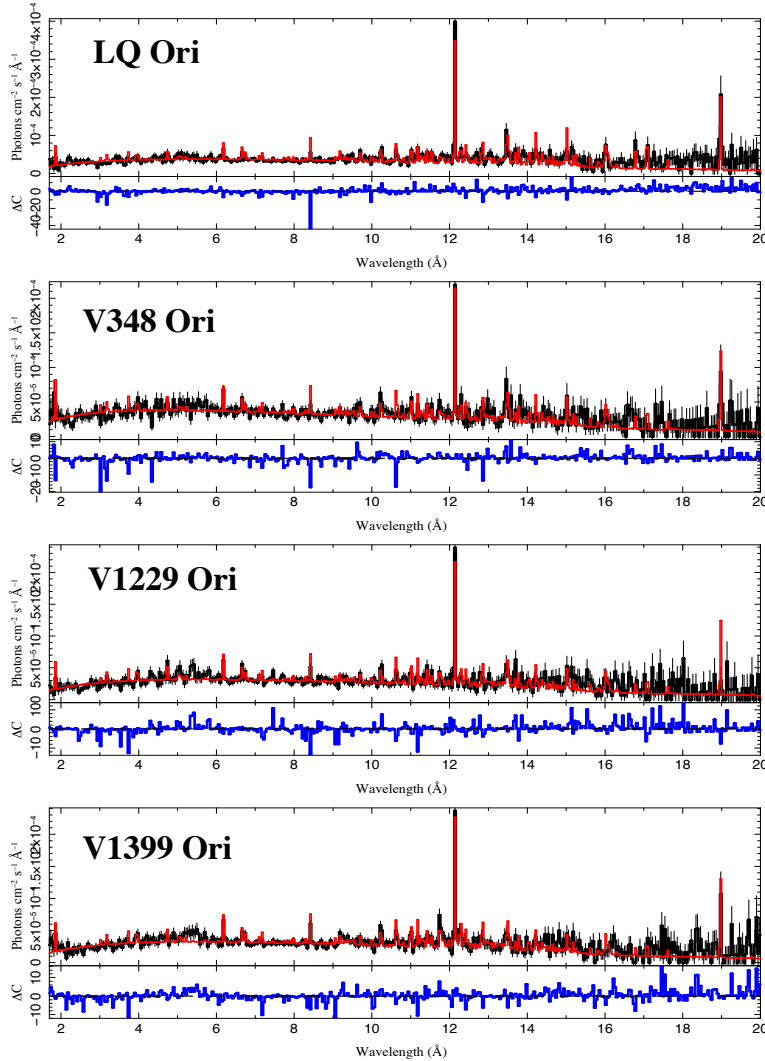


Figure 3: HETGS spectra of four T Tauri stars in the ONC (from Schulz et al. 2016). The spectra show strong Ne X and O VIII lines, some also strong Fe XXV lines indicating very hot coronal plasmas.

### References

Borosen et al. 2003, ApJ, 592, 516  
 Drake et al. 2015, ApJ, 802, 62  
 Hell et al. 2016, ApJ, submitted  
 House 1969, ApJS, 18, 21  
 Huenemoerder et al. 2015, ApJ, 815, 29  
 Kallman et al. 2014, ApJ, 780, 121  
 King et al. 2015, ApJ, 813, 37  
 Miller et al. 2016, ApJ, 821, 9  
 Miller et al. 2015, ApJ, 814, 87  
 Miskovicova et al. 2016, A&A, arXiv:1604.00364  
 Nardini et al. 2015, MNRAS, 453, 2558  
 Noble & Nowak 2008, PASP, 120, 821  
 Palmeri et al. 2008, ApJS, 177, 408  
 Phillips et al. 2015, ApJ, 809, 50  
 Schulz et al. 2015, ApJ, 810, 55  
 Schulz et al. 2002, ApJ, 564, 21  
 Watanabe et al. 2006, ApJ, 651, 421  
 Younes et al. 2015, 804, 43

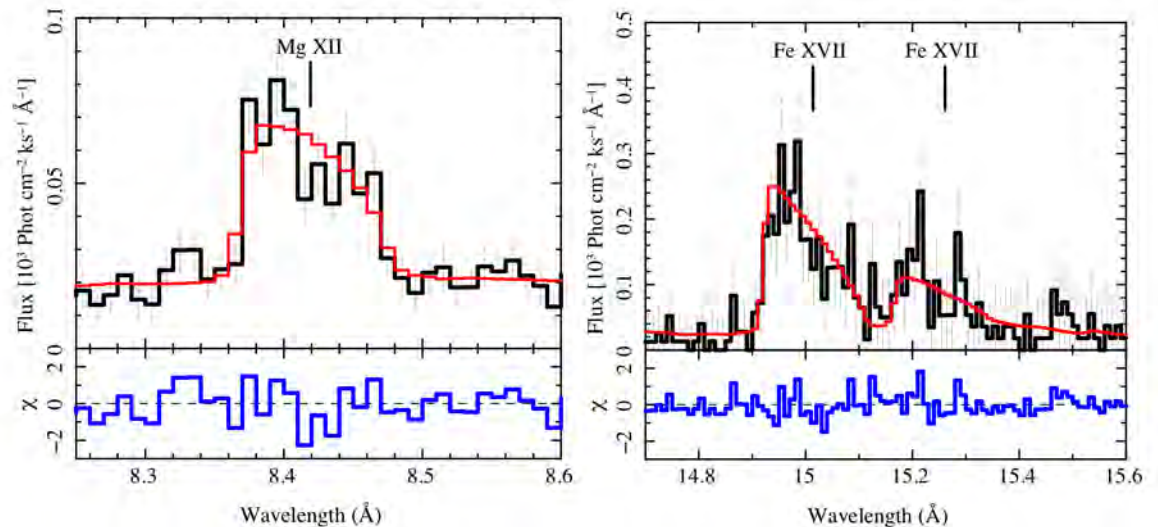


Figure 4: Model fits (red) to Mg XII (left) and Fe XVII (right) data (black) with residuals showing an unusual fin-like shape of the line profiles (from Huenemoerder et al. 2015).